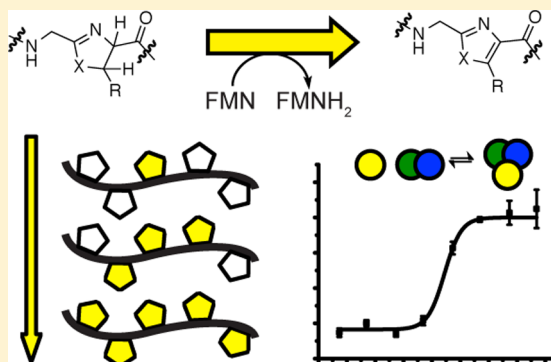


Orchestration of Enzymatic Processing by Thiazole/Oxazole-Modified Microcin Dehydrogenases

Joel O. Melby,^{†,‡} Xiangpo Li,^{†,‡} and Douglas A. Mitchell^{*,†,‡,§}[†]Department of Chemistry, [‡]Institute for Genomic Biology, and [§]Department of Microbiology; University of Illinois at Urbana–Champaign, Urbana, Illinois 61801, United States

S Supporting Information

ABSTRACT: Thiazole/oxazole-modified microcins (TOMMs) comprise a structurally diverse family of natural products with varied bioactivities linked by the presence of posttranslationally installed thiazol(in)e and oxazol(in)e heterocycles. The detailed investigation of the TOMM biosynthetic enzymes from *Bacillus* sp. Al Hakam (Balh) has provided significant insight into heterocycle biosynthesis. Thiazoles and oxazoles are installed by the successive action of an ATP-dependent cyclodehydratase (C- and D-protein) and a FMN-dependent dehydrogenase (B-protein), which are responsible for azoline formation and azoline oxidation, respectively. Although several studies have focused on the mechanism of azoline formation, many details regarding the role of the dehydrogenase (B-protein) in overall substrate processing remain unknown. In this work, we evaluated the involvement of the dehydrogenase in determining the order of ring formation as well as the promiscuity of the Balh and microcin B17 cyclodehydratases to accept a panel of noncognate dehydrogenases. In support of the observed promiscuity, a fluorescence polarization assay was utilized to measure binding of the dehydrogenase to the cyclodehydratase using the intrinsic fluorescence of the FMN cofactor. Ultimately, the noncognate dehydrogenases were shown to possess cyclodehydratase-independent activity. A previous study identified a conserved Lys–Tyr motif to be important for dehydrogenase activity. Using the tools developed in this study, the Lys–Tyr motif was shown neither to alter complex formation with the cyclodehydratase nor the reduction potential. Taken together with the known crystal structure of a homologue, our data suggest that the Lys–Tyr motif is of catalytic importance. Overall, this study provides a greater level of insight into the complex orchestration of enzymatic activity during TOMM biosynthesis.



TOMMs represent a subset of the larger ribosomally synthesized and post-translationally modified peptide class of natural products.¹ Characterized TOMMs feature a diverse range of biological activities including DNA gyrase inhibitors, translation inhibitors, and hemolytic toxins.^{1–5} The defining feature of TOMMs is the presence of thiazol(in)e and oxazol(in)e heterocycles derived from cysteine, serine, and threonine residues on a ribosomally produced precursor peptide.⁶ Thiazole and oxazole biosynthesis occurs over two steps, with the first being an ATP-dependent cyclodehydration to afford azoline heterocycles, which is catalyzed by the collective efforts of the C- and D-proteins (cyclodehydratase) encoded in TOMM biosynthetic gene clusters (Figure 1).^{7–10} Two-electron oxidation of the azoline by a FMN-dependent dehydrogenase (B-protein) affords the azole heterocycle.¹¹ In addition to these core modifications, many TOMMs contain a variety of other post-translational modifications catalyzed by ancillary enzymes found in the gene cluster.^{6,12–14}

Early studies on microcin B17 biosynthesis laid a foundation for understanding the mechanistic underpinnings of thiazole and oxazole installation.^{10,11,15} Although recent work has delved into the mechanistic enzymology and substrate-processing details of the Balh and cyanobactin cyclodehydratases, relatively

little is known regarding any potential role played by the dehydrogenase in orchestrating substrate processing.^{7–9,16–18} Upon its initial heterologous expression and copurification with a visibly yellow FMN cofactor, the B-protein was postulated to oxidize azolines to the corresponding azole.^{11,15} In microcin B17 biosynthesis, the dehydrogenase (McbC, whose letter designation derives from its position within the gene cluster, not its function) formed a complex with the cyclodehydratase (McbB and McbD) and proved to be an essential component for peptide processing.¹⁵ In contrast, the dehydrogenase has been shown to be dispensable for azoline formation with the Balh and cyanobactin cyclodehydratases.^{7,17,18} Using both native and artificial substrates, it was shown that the Balh cyclodehydratase (BalhC/D) cyclized particular cysteines, serines, and threonines (BalhA1, five cysteines; BalhA2, three cysteines and one threonine).^{16,17} However, the noncognate dehydrogenase from a highly similar biosynthetic gene cluster in *Bacillus cereus* 172560W, BcerB (78% identity/94% similarity

Received: November 13, 2013

Revised: December 22, 2013

Published: December 23, 2013



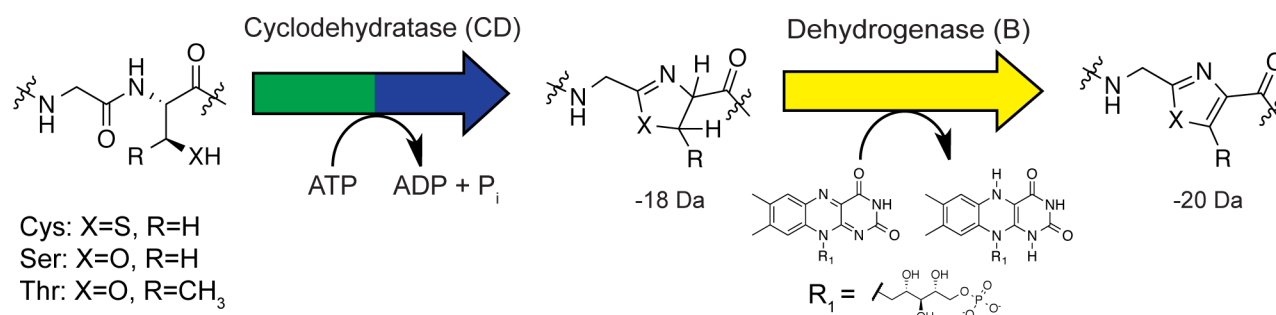


Figure 1. Synthesis of thiazole and oxazole heterocycles occurs over two distinct steps. First, the cyclodehydratase (C- and D-proteins) cyclizes cysteine, serine, or threonine residue into a thiazoline or oxazoline heterocycle through an ATP-dependent mechanism. Subsequently, a FMN-dependent dehydrogenase (B-protein) catalyzes the two-electron oxidation to the azole heterocycle, resulting in a 20 Da mass loss from the unmodified amino acid.

to BalhB, which purifies with minimal FMN cofactor), was capable of only oxidizing thiazolines.¹⁷ The chemoselectivity for thiazolines was reminiscent of the dehydrogenase involved in patellamide biosynthesis, which oxidizes two thiazolines while leaving two oxazolines intact.¹⁹ Another unique feature of the Balh TOMM was revealed upon determining the order of thiazole biosynthesis; processing by the BcrB/BalhC/BalhD complex occurred in an overall C- to N-terminal direction for the two substrates, BalhA1 and BalhA2 (Figure S1). Although this processing direction was unusual, it remained unclear if the cyclodehydratase or the dehydrogenase governed the order of ring formation.^{17,20}

Bioinformatic analyses have now identified over 1000 TOMM gene clusters, which are found by conducting BLAST searches using the C- or D-proteins as the query sequence. Owing to the sequence similarity of the TOMM dehydrogenase to other non-TOMM dehydrogenases, BLAST searches using the B-protein as the query sequence to identify new TOMM clusters suffer from a high false-positive rate. Frequently, TOMM clusters lack a dehydrogenase altogether (e.g., trunkamide²¹) and such products contain exclusively azoline heterocycles, not azoles. A rare exception to this rule is illustrated by bottromycin, whose biosynthetic gene cluster lacks any recognizable dehydrogenase.^{22–25} Instead, it is postulated that the oxidation of the sole thiazoline to the thiazole occurs via an oxidative decarboxylation, which is plausible given that the thiazole derives from the most C-terminal cysteine of the core region of the peptide (Figure S2).^{22,23,25} TOMM dehydrogenases belong to the nitroreductase superfamily (PFAM PF00881), which also includes FMN-dependent dehydrogenases involved in polyketide synthesis among other processes.^{26,27} TOMM dehydrogenases can be found as a single-domain protein or as a fusion to another protein involved in peptide maturation (e.g., PatG, involved in patellamide biosynthesis).^{28,29}

The ability of the Balh TOMM synthetase to exhibit cyclodehydratase and dehydrogenase activity independent of each other afforded the unique opportunity to explore the finer details of dehydrogenase activity. By decoupling cyclodehydratase and dehydrogenase activity, we were positioned to address long-standing questions regarding the individual roles of the cyclodehydratase and dehydrogenase in the order of substrate processing. Furthermore, the tolerance of noncognate dehydrogenases was explored in detail along with an investigation into the chemoselectivity of the dehydrogenase. Our study further implicates a previously identified Lys–Tyr motif, conserved among TOMM dehydrogenases, in catalysis.

EXPERIMENTAL PROCEDURES

General Methods. Unless otherwise specified, all chemicals were purchased from Fisher Scientific or Sigma-Aldrich. Oligonucleotides were purchased from Integrated DNA Technologies. Restriction enzymes were purchased from New England BioLabs (NEB). dNTPs were purchased from Genscript. Pfu Turbo DNA polymerase was purchased from Agilent. Sequencing grade trypsin was from Promega. DNA sequencing was performed by the Carver Biotechnology Center (University of Illinois at Urbana–Champaign) or ACGT, Inc.

Molecular Biology Techniques. The plasmids containing the Mcb and Balh/Bcr proteins were described previously.^{15,17} All other proteins were cloned into a modified pET28b plasmid containing MBP followed by a thrombin and TEV protease-cleavage sites, as described previously.³ In general, the dehydrogenases were amplified from genomic DNA using cloned Pfu DNA polymerase and the relevant primers (Table S1). The amplicons were then PCR-purified prior to a double restriction enzyme digest using *Bam*HI and *Not*I. After gel purification of the amplicons along with a similarly digested pET28b-MBP plasmid, the DNAs were ligated with T4 DNA Ligase (NEB). Site-directed mutagenesis was conducted using the QuikChange method (Agilent).

Overexpression and Purification of Fusion Proteins. All proteins were expressed and purified as fusions to maltose binding protein (MBP) as described previously.^{9,17} Proteolytic removal of MBP from was also performed as per previous reports.^{9,17}

General Synthetase Reactions. For Balh synthetase reactions, the precursor peptide (20–100 μ M), B-protein (0 or 5–50 μ M), C-protein (1–10 μ M), and D-protein (1–10 μ M) were combined in synthetase buffer (50 mM Tris, pH 7.4, 125 mM NaCl, 20 mM MgCl₂, 2 mM ATP, and 10 mM DTT) with concurrent TEV protease treatment to remove the MBP fusion partner (1 μ g of protease to 50 μ g of protein). Reactions were allowed to proceed for 16 h at 25 °C. In reactions containing the B-protein, FMN (50 μ M) was added to compensate for incomplete or inconsistent FMN loading during heterologous expression and purification. Precursor peptides containing only azoline heterocycles were generated from reactions that omitted the dehydrogenase. Synthetase reactions with the microcin B17 synthetase proteins were conducted in a similar fashion as in the case of Balh except that those reactions had 20 μ M McbA, 20 μ M dehydrogenase, 5 μ M McbB, and 5 μ M McbD.

Azoline Localization. Synthetase reactions lacking the B-protein (100 μ M BalhA1, 5 μ M BalhC, and 5 μ M BalhD) were

quenched after 30, 150, or 210 min by the addition of trypsin (1 μ g of trypsin to 25 μ g of total protein) for 1 h at 30 °C. Subsequently, iodoacetamide was added to a final concentration of 20 mM, and the labeling of uncyclized Cys residues was allowed to proceed for at least 30 min at 25 °C with minimal exposure to light. The samples were then acidified using formic acid (6% v/v), and the azolines were localized via LC–MS/MS as described below.

HPLC MS/MS. All reverse-phase LC–FTMS was performed using an Agilent 1200 HPLC system with an autosampler connected directly to a ThermoFisher Scientific LTQ–FT hybrid linear ion trap, operating at 11 T. The mass spectrometer was calibrated weekly following the manufacturer's protocol. Trypsin-digested samples were separated using a 1 \times 150 mm Jupiter C₁₈ column (300 Å, 5 μ M, Phenomenex). After a full scan detected in the FTMS, the MS/MS parent ions were manually selected, and ion detection was carried out in the ion-trap mass spectrometer. The following parameters were used: isolation width, 3 *m/z*; normalized collision energy, 35; activation *q* value, 0.25; and activation time, 30 ms. Data analysis was conducted using the Qualbrowser application of Xcalibur (Thermo-Fisher Scientific).

Determination of the Order of Azole Ring Formation. Generation of the pentathiazoline BalhA1 (BalhA1–STzn) was accomplished using synthetase reactions lacking the B-proteins (50 μ M BalhA1, 5 μ M BalhC, 5 μ M BalhD, and 1 μ g of TEV protease to 25 μ g of total protein). Upon complete formation of BalhA1–STzn (as judged by MALDI–TOF–MS), BcerB (5 μ M) and FMN (50 μ M) were then added to the reaction, which was allowed to proceed for either 4 or 45 min. Reactions were quenched by the addition of trypsin (1 μ g of trypsin to 25 μ g of total protein) for 1 h at 30 °C and subsequently acidified using formic acid (6% v/v) prior to HPLC MS/MS.

MALDI–TOF MS Analysis. All samples for MALDI–TOF–MS were desalted and concentrated by C₁₈ ZipTip (Millipore) according to the manufacturer's protocol. Samples were eluted in a saturated solution of CHCA matrix in 50:50 H₂O/ acetonitrile with 0.1% (v/v) trifluoroacetic acid. After the samples were allowed to dry under ambient conditions, they were analyzed using a Bruker Daltonics UltrafleXtreme MALDI–TOF/TOF using positive reflector mode. The instrument was calibrated using a peptide calibration kit (AB SCIEX). Data were analyzed using FlexAnalysis.

Fluorescence Polarization Assay for Dehydrogenase–Cyclodehydratase Complexation. Fluorescence polarization was conducted using a FilterMax F5 multi-mode microplate reader (Molecular Devices). The dehydrogenase (1 μ M) and varying concentration of the C- and D-proteins were added to a 384-well black polystyrene microplate (Corning) and allowed to equilibrate for 30 min prior to measurement. For all samples, the autofluorescence of the C- and D-proteins were used for background correction. A sigmoidal dose–response curve fitting was conducted using OriginPro9.

Measurement of TOMM Dehydrogenase Reduction Potentials. The reduction potential for various TOMM dehydrogenases were determined as described by Massey.³⁰ The dehydrogenase (300 μ M BcerB and 100 μ M other dehydrogenases), benzyl viologen (2 μ M), and phenosafranine (10 μ M) were added to a 10 mL round-bottomed flask, and the final volume was brought to 2 mL using protein storage buffer (50 mM HEPES, pH 7.5, 0.3 M NaCl, and 2.5% glycerol (v/

v)). The protein solution was degassed using a Schlenk line and subsequently introduced into an anaerobic chamber where the protein was allowed to equilibrate for 30 min while stirring. UV–vis spectra were acquired using an Agilent 8453 spectrometer (Agilent Technologies). Sodium dithionite (1–5 μ L of 10 mM) was employed to reduce chemically FMN and phenosafranine. After sodium dithionite addition, the solution was stirred for 5 min prior to recording another UV–vis spectrum. This process was repeated until both FMN and phenosafranine were fully reduced. Using the absorbance measurements of FMN (440–450 nm) and phenosafranine (520 nm), a plot of log(ox/red) phenosafranine versus log(ox/red) dehydrogenase was used to calculate the reduction potential of the dehydrogenases.

RESULTS

Order of Azoline and Azole Ring Formation. Azole formation by the Balh TOMM synthetase proceeds in an overall C- to N-terminal direction.¹⁷ An unresolved question was whether this processing direction was governed by the cyclodehydratase, the dehydrogenase, or by their collaboration. Because of chemical instability, routine LC–MS/MS cannot be employed to localize peptidic azolines because such heterocycles rapidly hydrolyze and revert to the unmodified amino acid.^{31,32} As an alternative approach, any unprocessed cysteines could be labeled using iodoacetamide, which would then be distinguishable from processed cysteines by LC–MS/MS.^{20,33} To generate azoline intermediates, the BalhA1 precursor peptide was treated with the BalhC/D cyclodehydratase (dehydrogenase omitted). After a specified time, the reactions were quenched by the addition of trypsin, and the unmodified cysteines were labeled with iodoacetamide. Subsequent acidification with formic acid hydrolyzed all thiazolines to cysteine. The modified and unmodified cysteines were then identified using LC–MS/MS (Figure 2). By this method, residues that were converted to thiazolines would be detected as an unmodified cysteine, whereas the residues labeled by iodoacetamide would indicate cysteines that did not undergo cyclodehydration. The order of azoline formation precisely followed the overall order of azole formation previously determined when the substrate was treated with the full consortium of TOMM synthetase proteins (BCD together).¹⁷ Irrespective of the presence of the dehydrogenase, Cys40 was cyclized first followed by Cys31 and Cys34 in equal amounts, Cys45, and finally, Cys28 (Figure 3).

The ability to decouple cyclodehydratase and dehydrogenase activity not only allowed the investigation of azoline order but also permitted the dissection of azole order of the dehydrogenase, BcerB. Upon adding BcerB to the pentathiazoline of BalhA1 (BalhA1–STzn, preformed by BalhC/D), the order of oxidations en route to BalhA1–STzn could be monitored as in previous studies using LC–MS/MS.¹⁷ Intriguingly, the processing order failed to follow azoline biogenesis. The first position to be oxidized was Tzn34 followed by an outward series of modifications simultaneously radiating toward the N- and C-termini (Figure 4).

Permissive Nature of TOMM Dehydrogenases. As we have noted in our earlier reports,^{9,17} the BalhB dehydrogenase purifies with minimal bound FMN cofactor (predominately apo); thus, the above studies were conducted using a noncognate dehydrogenase from *Bacillus cereus* 172560W. Dubbed BcerB, this protein copurifies with FMN and shares significant sequence similarity with BalhB (78% identity/94%

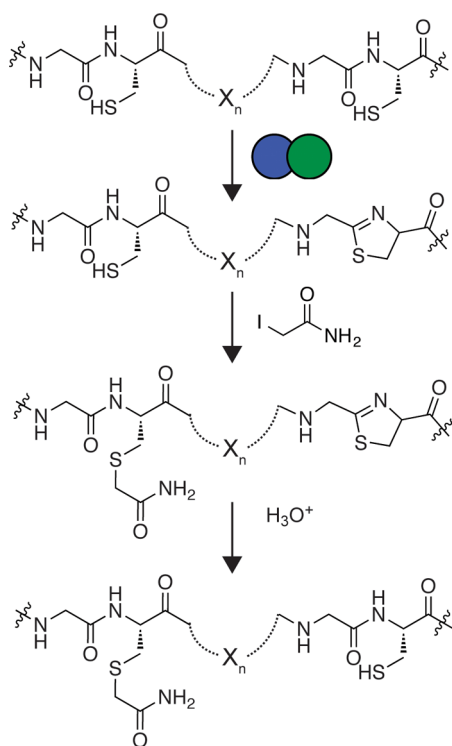


Figure 2. Iodoacetamide labeling for azoline localization. In an ordered fashion, the cyclodehydratase installs azoline heterocycles onto the precursor peptide. Cysteines that have not undergone cyclodehydration were labeled with iodoacetamide. Acid-catalyzed hydrolysis reverts thiazolines back to cysteines. Localizing the unmodified and acetamide-labeled cysteines allowed the order of processing to be determined.

similarity).^{9,17} It has also been shown with the TOMM from *Clostridium botulinum* that a noncognate dehydrogenase, SagB from *Streptococcus pyogenes* (41% identity/80% similarity to ClosB), can successfully substitute for the cognate dehydrogenase, ClosB, during in vitro reconstitution of clostridiolysin S.³⁴

In both of the cases mentioned above, the substituted dehydrogenase was closely related to the cognate dehydrogenase. To test the ability of more distant dehydrogenases to successfully complement thiazole/oxazole biosynthesis, a series of diverse dehydrogenases were cloned, expressed, purified, and tested for activity using the Balh and Mcb TOMM cyclodehydratases (Table S2 and Figures 5, 6, and S1). All noncognate dehydrogenases formed thiazoles in conjunction with the Balh cyclodehydratase (Figure 5). The order of azole formation was also determined for reactions containing the TOMM dehydrogenases from *Bacillus amyloliquefaciens* FZB42 and *Clavibacter michiganensis* subsp. *sepedonicus* (BamB and CmsB, respectively). Both dehydrogenases followed a highly similar pathway as BcerB when processing BalhA1-5Tzn (Figures 4 and S3). In stark contrast to the flexible nature of the Balh enzymes, only reactions with the cognate dehydrogenase (McbC) produced heterocycles when testing the Mcb cyclodehydratase (McbB/D). The observed dehydrogenase intolerance of the Mcb cyclodehydratase suggests that the noncognate dehydrogenases tested are not capable of forming a productive trimeric complex with McbB/D, which has been shown to be essential for thiazole/oxazole biosynthesis.¹⁵

Monitoring TOMM Synthetase Complex Formation by Fluorescence Polarization. Because noncognate dehydrogenases successfully oxidized BalhA1 in the presence of BalhC/D, whereas all of the dehydrogenases (except McbC) tested failed to complement McbB/D, we hypothesized that the dehydrogenases might be able to form a complex with BalhC/D but not with McbB/D. To test this, we utilized a fluorescence polarization-based binding assay that capitalizes on the intrinsic fluorescence of the FMN cofactor. A similar assay has been employed to study the interaction of luciferase and lumazine.^{35,36} An increase in the fluorescence polarization would occur upon binding of the dehydrogenase to the cyclodehydratase complex. Fluorescence polarization was measured using a fixed concentration of BcerB with increasing concentrations of BalhC/D (Figure 7). As the concentrations

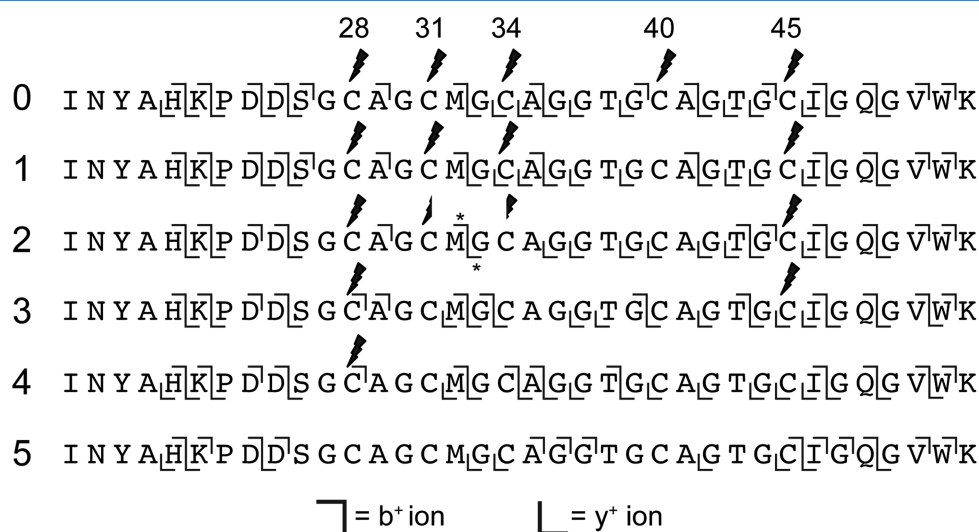


Figure 3. MS/MS fragmentation of BalhA1 azoline intermediates. BalhA1 reactions with BalhC/D to produce thiazoline-containing intermediates were treated with trypsin and iodoacetamide to identify unreacted cysteines. Subsequent addition of formic acid returned all thiazolines back to cysteine, at which point the samples were subjected to LC-FTMS/MS. The fragment ions observed for various ring intermediates are denoted by the b⁺ and y⁺ ion symbols. The leftmost numbers indicate ring state. Across the top, cysteines are numbered on the basis of the sequence of full-length BalhA1. Lightning bolts signify locations labeled with iodoacetamide. Asterisks denote ions containing a mixed population of two peptides.

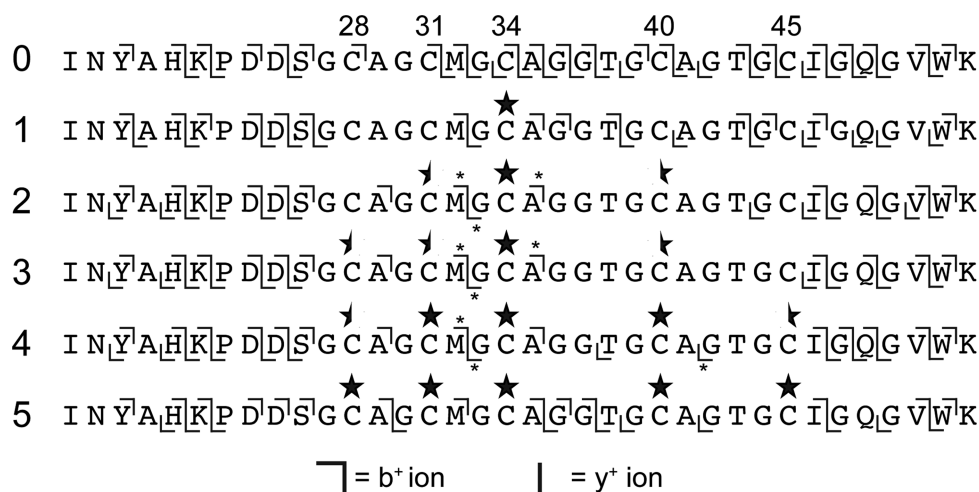


Figure 4. MS/MS fragmentation of BalhA1 azole intermediates. Synthetase reactions containing BalhA1-5Tzn treated with BcerB were quenched by the addition of trypsin and subjected to LC-FTMS/MS. The fragment ions observed for various ring intermediates are denoted by the b⁺ and y⁺ ion symbols. The leftmost numbers indicate ring state. Across the top, cysteines are numbered on the basis of the sequence of full-length BalhA1. Stars signify thiazole locations, whereas a half-star signifies that there are ions indicative of a thiazole as well as a free cysteine at that position. Asterisks denote ions containing a mixed population of two peptides.

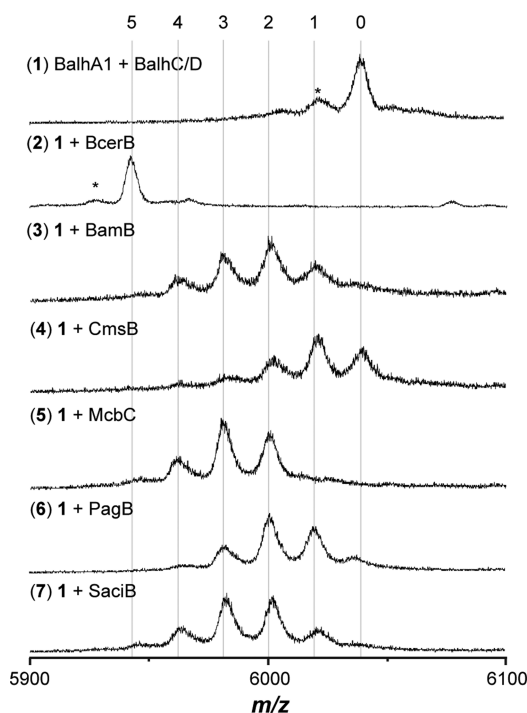


Figure 5. Balh cyclodehydratase tolerates noncognate dehydrogenases. The reactions containing the indicated reagents were allowed to react for 16 h at 25 °C and then analyzed using MALDI-TOF-MS after formic acid hydrolysis of thiazoline heterocycles. The numbers at the top indicate the number of azole heterocycles. The asterisks denote a laser-induced artifact.

of BalhC/D were increased, significant fluorescence polarization was observed, and the apparent K_d of $1.7 \pm 0.2 \mu\text{M}$ aligned with the previously reported K_{complex} measured for McbC to McbB/D ($1.8 \pm 0.8 \mu\text{M}$).¹⁵ All other noncognate dehydrogenases were also subjected to this binding assay, yet no binding was observed (data not shown).

Cyclodehydratase-Independent Dehydrogenation. To reconcile the dehydrogenase activity observed in the absence of detectable binding of noncognate dehydrogenases (with the

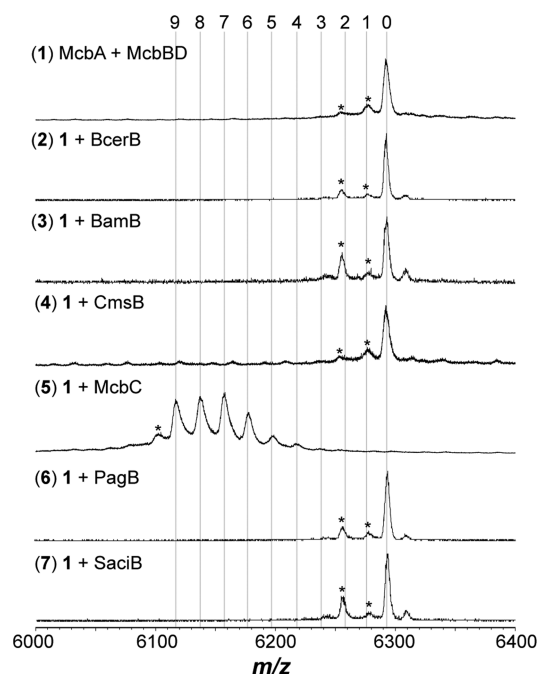


Figure 6. Dehydrogenase intolerance of the Mcb cyclodehydratase. The reactions containing the indicated reagents were allowed to react for 16 h at 25 °C and then analyzed using MALDI-TOF-MS after formic acid hydrolysis of azoline heterocycles. The numbers at the top indicate the number of azole heterocycles. The asterisks denote a laser-induced artifact.

exception of BcerB) to BalhC/D, the ability of such dehydrogenases to act upon BalhA1-5Tzn in a cyclodehydratase-independent fashion was measured. Initially, the requirements for efficient dehydrogenation were monitored using BcerB. After forming BalhA1-5Tzn with BalhC/D and concomitant TEV cleavage, acetonitrile was added to the reaction mixture to precipitate large proteins while leaving BalhA1-5Tzn in solution. After centrifugation, decantation, and evaporation of the acetonitrile supernatant by vacuum centrifugation, various combinations of BcerB, BalhC, and

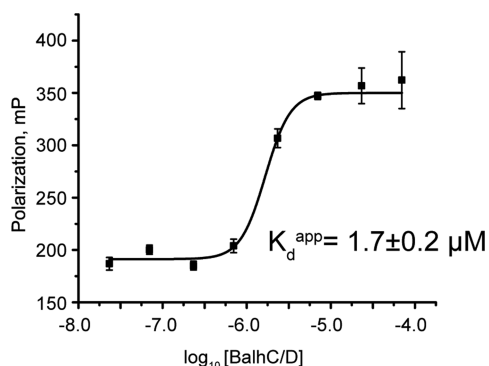


Figure 7. Fluorescence polarization of BcerB and the Balh cyclodehydratase. The fluorescence polarization of the FMN cofactor of BcerB (1 μ M) was measured with varying concentrations of the Balh cyclodehydratase. A dose–response fit of the data provided the apparent K_d . The error reported for each individual data point corresponds to the standard deviation of three technical replicates, whereas the error reported for the apparent K_d derives from the error associated with curve fitting.

BalhD were added (Figure S4). As a control, addition of BalhA1 to these samples did not result in any detectable enzymatic processing, indicating that the acetonitrile-based removal of BalhC/D was adequate and any residual enzymes were inactive (Figure S4). To deconvolute the mixture of heterocycles, formic acid was added to hydrolyze selectively the thiazolines, leaving thiazoles intact (Figure 8).^{16,37} From these experiments, it became clear that dehydrogenation efficiently occurred only when the dehydrogenase was present with both cyclodehydratase proteins (i.e., BalhC/D), although thiazoline oxidation intermediates were observed when individual components of the cyclodehydratase were supplied separately

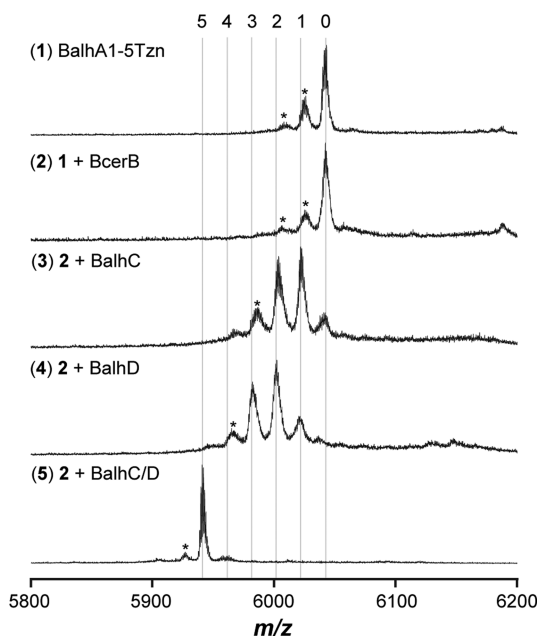


Figure 8. Minimal requirement for dehydrogenase activity. BalhA1-5Tzn was treated with varying combinations of synthetase components. The reactions were allowed to react for 16 h at 25 $^{\circ}$ C and then analyzed using MALDI-TOF-MS after formic acid hydrolysis of thiazoline heterocycles. The numbers above the spectra indicate the number of azole heterocycles. Asterisks denote laser-induced artifacts.

(Figure 8). The cyclodehydratase-independent activity was then measured using the entire panel of noncognate dehydrogenases (Figure S5). Contrary to BcerB, all other noncognate dehydrogenases exhibited roughly the same processing efficiency, regardless of the presence of BalhC/D (Figures 5 and S5).

Universal Importance of the Conserved Lys–Tyr Motif in TOMM Dehydrogenases. Sequence alignment of TOMM dehydrogenases reveals a highly conserved Lys–Tyr motif (Figure S6).¹⁶ On the basis of Protein DataBank entry 3EO7 (a putative nitroreductase from *Anabaena variabilis* ATCC 29413), which is the most similar protein with a published structure (12% identity/51% similarity to McbC), the Lys–Tyr motif is located near the FMN cofactor (closest distance is 5.6 Å, Figure S7). Mutagenesis of the Lys–Tyr motif failed to alter the FMN loading, further suggesting that the Lys–Tyr motif is not directly involved in FMN binding (Figure S8). A previous study, which replaced the Lys201 and Tyr202 of McbC to Ala, resulted in inactive protein during microcin B17 in vitro reconstitution reactions, suggestive of a potential catalytic role.¹⁶ McbC-K201A and -Y202A were also inactive toward BalhA1-5Tzn (Figure S9). The equivalent Lys–Tyr motifs in the TOMM dehydrogenases from the Gram-positive *Bacillus cereus* 172560W (BcerB) and the thermoacidophilic archaeon *Sulfolobus acidocaldarius* DSM 639 (SaciB) were mutated to Ala and screened for activity. BcerB-K185A exhibited reduced activity, as indicated by the formation of up to four thiazoles in an end-point assay, whereas BcerB-Y186A and the double mutant (K185A/Y186A) were catalytically inactive (Figure 9). Similar to McbC, the single and double mutants to the Lys–Tyr motif in SaciB abolished activity (Figure 9). Increased protein concentrations (5–50 μ M dehydrogenase) and reaction times (24 h) failed to restore detectable activity for the BcerB, SaciB, and McbC mutants. In further support for a catalytic role, BcerB-K185A and -Y186A were tested for their ability to form a complex with BalhC/D. Using the FMN-based fluorescence polarization assay, BcerB-K185A/Y186A was found to bind with similar affinity as wild-type BcerB (Figure S10). Taken together, our data suggest that the Lys–Tyr motif plays a role in catalysis by the dehydrogenase.

Comparison of TOMM Dehydrogenase Reduction Potentials. It was shown previously that although BcerB was an efficient thiazoline oxidase, this protein was unable to convert oxazolines to oxazoles, irrespective of the presence of BalhC/D.¹⁷ A possible explanation for the lack of activity toward oxazolines could arise from a difference in reduction potential compared to other B-proteins that produce oxazoles. To measure reduction potentials, UV–vis spectra were collected while the FMN cofactor was chemically reduced using sodium dithionite (Figure S11). Addition and subsequent monitoring of the redox indicator dye, phenosafranine, allowed calculation of the dehydrogenase reduction potentials.³⁰ Using this method, initial studies were focused on BcerB and McbC (oxidizes four oxazolines during microcin B17 maturation), which gave identical reduction potentials (Table 1).¹¹ The reduction potential of BamB provided further evidence that BcerB does not harbor significantly different electrochemical properties compared to other TOMM dehydrogenases and as such, does not explain the observed selectivity toward thiazolines. Similarly, an altered reduction potential of the Lys–Tyr mutants could provide an explanation for the dearth of catalytic activity observed. However, the reduction potential of McbC-Y202A was not statistically different from BcerB

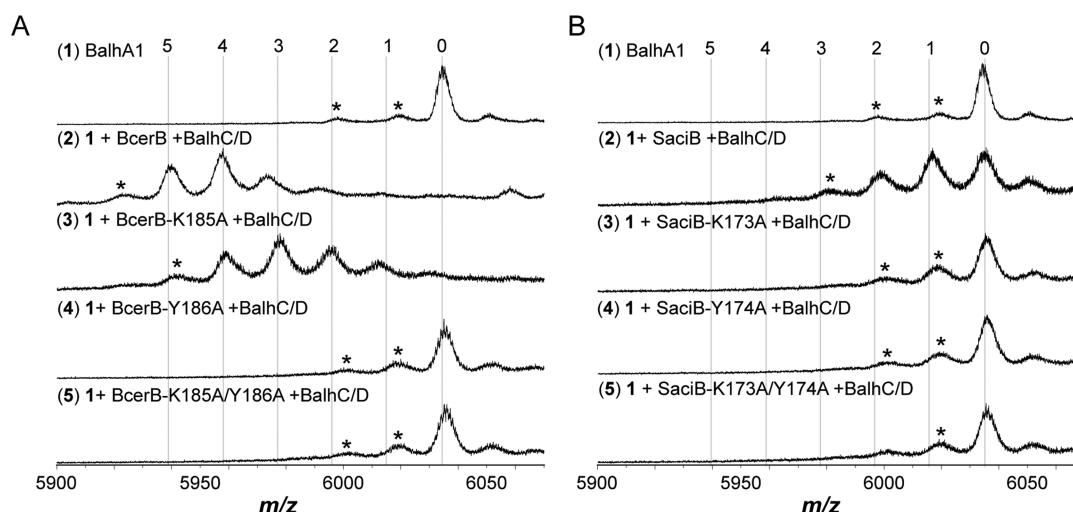


Figure 9. Dehydrogenase activity of Lys–Tyr mutants. (A) Synthetase reactions containing BcerB and the indicated mutants were conducted and allowed to react for 16 h at 25 °C. Subsequently, all azoline heterocycles were hydrolyzed using formic acid prior to MALDI-TOF-MS analysis. (B) Same as panel A except that the reactions contained SaciB and its Lys–Tyr mutants. The numbers above the spectra indicate the number of azole heterocycles. The asterisks denote laser-induced artifacts.

Table 1. Reduction Potentials of TOMM Dehydrogenases^a

protein	redox potential (mV)
BcerB	−277 ± 4
McbC	−277 ± 2
BamB	−280 ± 3
McbC Y202A	−272 ± 1

^aThe redox potential of the listed TOMM dehydrogenases were measured by chemically reducing the FMN cofactor with sodium dithionite in the presence of phenosafranine, an indicator dye, and monitoring the reduction of both by UV–vis spectroscopy.³⁰ The error reported is the standard deviation of three independent measurements.

(Table 1), further implicating the Lys–Tyr motif in enzymatic catalysis (Figure S2).

DISCUSSION

During microcin B17 biosynthesis, the full trimeric complex of McbBCD is required for thiazole/oxazole ring formation.¹⁵ Fortunately, the cyclodehydratase from Balh does not require the dehydrogenase for activity, which allowed us to examine cyclodehydration separately from dehydrogenation. Although the order of thiazoline formation by BalhC/D (Figure 3) followed the previously reported order for azole formation (generated from a full BCD reaction), the order of azole formation when the dehydrogenase was presented with a pentaazoline substrate (BalhA1-5Tzn) proved drastically different. During BalhA1-5Tzn processing, BcerB first oxidized the thiazoline at Cys34 (Tzn34) and subsequently proceeded outward toward the C- and N-termini simultaneously (Figure 4). Other dehydrogenases processed the BalhA1-5Tzn substrate in a similar fashion (Figure S3). A potential explanation could be that the dehydrogenases recognize a specific motif within the precursor peptide, which, on the basis of distance constraints, orients Tzn34 closest to the active site. However, both the microcin B17 and streptolysin S TOMM dehydrogenases (McbC and SagB, respectively) were shown to have little affinity for their cognate precursor peptides.^{15,38} The aberrant order of cyclodehydratase-independent dehydrogenase activity also demonstrated that although BalhA1-5Tzn was a

competent intermediate, it did not follow the native biosynthetic processing order. When the full biosynthetic complex was present, azole order proceeded in an overall C- to N-terminal direction and exhibited a distributive behavior, which was determined by the detection of intermediates with varying numbers of thiazole heterocycles.¹⁷ As such, we propose a biosynthetic pathway where dehydrogenation immediately follows cyclodehydration at every modified position.

The ability of noncognate dehydrogenases to substitute for the native dehydrogenase does not appear to be universal in TOMM biosynthesis. With the Balh cyclodehydratase, every dehydrogenase tested could install thiazoles onto the BalhA1 substrate in the presence of BalhC/D (Figure 5), but only the native McbC dehydrogenase was tolerated during McbA processing (Figure 6). During in vitro reconstitution of microcin B17 biosynthesis, the three McbBCD proteins are each essential; omission of any protein abrogates all detectable enzymatic activity.¹⁵ Coimmunoprecipitation studies demonstrated that McbBCD form a heterotrimeric complex in which each component performs a unique function during azole formation.^{9,11} Therefore, if a noncognate dehydrogenase fails to form a productive heterotrimeric complex with McbB/D (cyclodehydratase) successfully, no heterocycle formation would be expected to occur. The ability of the noncognate dehydrogenases to complement the Balh cyclodehydratase suggested that a catalytically active trimeric complex was formed between the dehydrogenases and cyclodehydratase. To provide evidence for complex formation between noncognate dehydrogenases and the Balh cyclodehydratase, a fluorescence polarization assay utilizing the intrinsic fluorescence of the FMN cofactor was employed to monitor binding. Surprisingly, only BcerB, a dehydrogenase from a nearly identical biosynthetic gene cluster, in conjunction with BalhC/D produced a fluorescence polarization curve indicative of complex formation (Figure 7). The instability of McbBCD at a high concentration without their MBP fusion partner precluded the monitoring of fluorescence polarization between McbC and McbB/D. The inability to detect an increase in fluorescence polarization using noncognate dehydrogenases

suggested that there was cyclodehydratase-independent dehydrogenase activity.

To garner further support for the dehydrogenase activity in the absence of a cyclodehydratase, we monitored dehydrogenase activity toward BalhA1-5Tzn in the absence of BalhC/D. To prepare this substrate, synthetase reactions were initiated with BalhA1 and BalhC/D. After completion of the reaction, acetonitrile was added to precipitate large polypeptides (i.e., BalhC and BalhD) while leaving BalhA1 derivatives in solution. After removal of the acetonitrile, BalhA1-5Tzn was subjected to various enzymatic reactions. As expected, efficient dehydrogenation occurred only when all of the biosynthetic enzymes were added (BCD), but a minimal amount of activity was detected when BcerB was present with either BalhC or BalhD (Figure 8). BcerB alone had no detectable activity when presented with BalhA1-5Tzn (Figures 8 and S4). However, the other TOMM dehydrogenases were able to catalyze azole formation in the absence of BalhC/D (Figure S5). This result provided an explanation for the inability to detect binding between the noncognate dehydrogenases (with the exception of BcerB) and BalhC/D while still being able to catalyze azole formation (Figure S5). It appears that all of the dehydrogenases tested, excluding BcerB, exhibit nonspecific azoline oxidation.

A previous study identified a conserved Lys–Tyr motif (Figure S6) that abolished the dehydrogenase activity of McbC.¹⁶ In the process of evaluating the biochemical determinants of azoline oxidation, the importance of the Lys–Tyr motif was further established in two other distantly related TOMM dehydrogenases (BcerB and SaciB). Mutation of either the Lys or the Tyr within the SaciB motif eradicated enzymatic activity in our assays (Figure 9). In BcerB, the K185A mutation had reduced activity as indicated by the detection of predominantly a three thiazole heterocycle species of BalhA1. However, BcerB-Y186A and -K185A/Y186A were devoid of activity (Figure 9). In all cases, mutation of the Lys–Tyr motif did not alter the FMN content of the dehydrogenase (Figure S8). Using the fluorescence polarization assay, BcerB-K185A/Y186A was found to form a complex with BalhC/D (Figure S10), indicating that the Lys–Tyr motif did not play a critical role in the protein–protein interaction. Another possible explanation for the loss of activity was an altered reduction potential; however, the potentials of McbC-Y202A and BcerB were not significantly different ($p > 0.1$). On the basis of the crystal structure of the closest homologue (PDB: 3EO7), it appeared the Lys–Tyr motif was poised to participate in catalysis, given its proximity to the active site (Figures S2 and S7). Taken together with our fluorescence polarization assays, FMN loading, and electrochemical titrations, the loss of activity in three distinct TOMM dehydrogenases supports a catalytic role for these residues (Figure S2).¹⁶ A more detailed kinetic analysis of the Lys–Tyr mutants will be necessary to establish unequivocally a catalytic role for these residues.

Interestingly, the Balh cyclodehydratase can cyclize cysteine, serine, and threonine residues to their respective azoline heterocycles,^{16,17} yet BcerB lacks the capability to convert (methyl)oxazolines to (methyl)azoles. Owing to the greater aromatic character of a thiazole relative to an oxazole, the oxidation of a thiazoline is more thermodynamically favorable than oxazoline oxidation.³⁹ Therefore, one way to oxidize thiazolines chemoselectively would be to tune finely the electrochemical potential of the dehydrogenase. However, our measurement of TOMM dehydrogenase reduction potentials

fails to explain the observed chemoselectivity of BcerB, as the values measured were not significantly different than dehydrogenases known to form oxazoles (Table 1). The observed chemoselectivity must then derive from the ability of BcerB to discriminate between thiazolines and oxazoline by some other mechanism. A possible explanation is a difference in pK_a between the α -hydrogens of a thiazoline versus an oxazoline. Base-catalyzed removal of the α -hydrogen may be rate-determining in dehydrogenation reactions (Figure S2).¹¹

In conclusion, the ability to discriminate between cyclodehydratase and dehydrogenase function afforded the opportunity to study the order of both azoline and azole ring formation, which, in the case of Balh, was dictated by the cyclodehydratase. Testing the limit of noncognate dehydrogenase swapping with the Balh cyclodehydratase demonstrated that most noncognate dehydrogenases do not bind the Balh cyclodehydratase and nonspecifically oxidize the azoline-containing substrate. Furthermore, a conserved Lys–Tyr motif within the dehydrogenase was found to be critical for activity in distantly related TOMM dehydrogenases, which is postulated to play a role in acid/base catalysis. Through measurement of the reduction potential of a panel of dehydrogenases, the chemoselectivity of BcerB for thiazoline heterocycles does not result from a tuned redox potential and instead discriminates thiazoline from oxazoline at the substrate level.

■ ASSOCIATED CONTENT

● Supporting Information

Oligonucleotides used in this study; bioinformatic data for the dehydrogenases used in this study; dehydrogenase identity/similarity matrix and amino acid sequence of precursor peptides; three potential pathways for azole formation in ribosomal natural product biosynthesis; order of azole formation on BalhA1-5Tzn by CmsB and BamB; minimal requirement for dehydrogenase activity; noncognate dehydrogenase activity towards BalhA1-5Tzn; TOMM dehydrogenase alignment; non-TOMM dehydrogenase crystal structure highlighting the Lys–Tyr motif; UV–vis of dehydrogenases; McbC-K201A and -Y202A lack dehydrogenase activity; binding of BcerB-K185A/Y186A to BalhC/D; and reduction potential of McbC measured by phenosafranine titration. This material is available free of charge via the Internet at <http://pubs.acs.org>.

■ AUTHOR INFORMATION

Corresponding Author

*E-mail: douglasm@illinois.edu; Phone: 1-217-333-1345; Fax: 1-217-333-0508.

Funding

This work was supported by the U.S. National Institutes of Health (NIH) (1R01 GM097142 to D.A.M.). X.L. was in part supported by a fellowship from the Department of Chemistry at the University of Illinois at Urbana–Champaign. The Bruker UltrafleXtreme MALDI TOF/TOF mass spectrometer was purchased in part with a grant from the National Center for Research Resources, National Institutes of Health (S10 RR027109 A).

Notes

The authors declare no competing financial interest.

ACKNOWLEDGMENTS

We are grateful for the gift of *Clavibacter michiganensis* subsp. *sepedonicus* from Carol Ishimaru (University of Minnesota). We thank Kyle Dunbar, Courtney Cox, Robbie Downen, and Joyce Limm for technical assistance. Members of the Mitchell Lab carried out critical review of this manuscript.

ABBREVIATIONS USED

ATP, adenosine-5'-triphosphate; Balh, *Bacillus* sp. Al Hakam; CHCA, α -cyano-4-hydroxycinnamic acid; CV, column volumes; DTT, dithiothreitol; FMN, flavin mononucleotide; HEPES, 2-[4-(2-hydroxyethyl)piperazin-1-yl]ethanesulfonic acid; IPTG, isopropyl- β -D-thiogalactopyranoside; LC-FTMS, liquid chromatography–Fourier transform mass spectrometry; MALDI-TOF-MS, matrix-assisted laser desorption/ionization time-of-flight mass spectrometry; MBP, maltose-binding protein; TEV, tobacco etch virus; TOMM, thiazole/oxazole-modified microcin

REFERENCES

- (1) Arnison, P. G., Bibb, M. J., Bierbaum, G., Bowers, A. A., Bugni, T. S., Bulaj, G., Camarero, J. A., Campopiano, D. J., Challis, G. L., Clardy, J., Cotter, P. D., Craik, D. J., Dawson, M., Dittmann, E., Donadio, S., Dorrestein, P. C., Entian, K. D., Fischbach, M. A., Garavelli, J. S., Goransson, U., Gruber, C. W., Haft, D. H., Hemscheidt, T. K., Hertweck, C., Hill, C., Horswill, A. R., Jaspars, M., Kelly, W. L., Klinman, J. P., Kuipers, O. P., Link, A. J., Liu, W., Marahiel, M. A., Mitchell, D. A., Moll, G. N., Moore, B. S., Muller, R., Nair, S. K., Nes, I. F., Norris, G. E., Olivera, B. M., Onaka, H., Patchett, M. L., Piel, J., Reaney, M. J., Rebuffat, S., Ross, R. P., Sahl, H. G., Schmidt, E. W., Selsted, M. E., Severinov, K., Shen, B., Sivonen, K., Smith, L., Stein, T., Sussmuth, R. D., Tagg, J. R., Tang, G. L., Truman, A. W., Vederas, J. C., Walsh, C. T., Walton, J. D., Wenzel, S. C., Willey, J. M., and van der Donk, W. A. (2013) Ribosomally synthesized and post-translationally modified peptide natural products: overview and recommendations for a universal nomenclature. *Nat. Prod. Rep.* 30, 108–160.
- (2) Molloy, E. M., Cotter, P. D., Hill, C., Mitchell, D. A., and Ross, R. P. (2011) Streptolysin S-like virulence factors: The continuing saga. *Nat. Rev. Microbiol.* 9, 670–681.
- (3) Lee, S. W., Mitchell, D. A., Markley, A. L., Hensler, M. E., Gonzalez, D., Wohlrab, A., Dorrestein, P. C., Nizet, V., and Dixon, J. E. (2008) Discovery of a widely distributed toxin biosynthetic gene cluster. *Proc. Natl. Acad. Sci. U.S.A.* 105, 5879–5884.
- (4) Vizán, J. L., Hernandez-Chico, C., del Castillo, I., and Moreno, F. (1991) The peptide antibiotic microcin B17 induces double-strand cleavage of DNA mediated by *E. coli* DNA gyrase. *EMBO J.* 10, 467–476.
- (5) Bagley, M. C., Dale, J. W., Merritt, E. A., and Xiong, X. (2005) Thiopentide antibiotics. *Chem. Rev.* 105, 685–714.
- (6) Melby, J. O., Nard, N. J., and Mitchell, D. A. (2011) Thiazole/oxazole-modified microcins: Complex natural products from ribosomal templates. *Curr. Opin. Chem. Biol.* 15, 369–378.
- (7) Koehnke, J., Bent, A. F., Zollman, D., Smith, K., Houssen, W. E., Zhu, X., Mann, G., Lebl, T., Scharff, R., Shirran, S., Botting, C. H., Jaspars, M., Schwarz-Linek, U., and Naismith, J. H. (2013) The cyanobactin heterocyclase enzyme: A processive adenylase that operates with a defined order of reaction. *Angew. Chem.* 125, 14241–14246.
- (8) McIntosh, J. A., and Schmidt, E. W. (2010) Marine molecular machines: Heterocyclization in cyanobactin biosynthesis. *ChemBioChem* 11, 1413–1421.
- (9) Dunbar, K. L., Melby, J. O., and Mitchell, D. A. (2012) YcaO domains use ATP to activate amide backbones during peptide cyclodehydrations. *Nat. Chem. Biol.* 8, 569–575.
- (10) Milne, J. C., Eliot, A. C., Kelleher, N. L., and Walsh, C. T. (1998) ATP/GTP hydrolysis is required for oxazole and thiazole

biosynthesis in the peptide antibiotic microcin B17. *Biochemistry* 37, 13250–13261.

(11) Li, Y. M., Milne, J. C., Madison, L. L., Kolter, R., and Walsh, C. T. (1996) From peptide precursors to oxazole and thiazole-containing peptide antibiotics: Microcin B17 synthase. *Science* 274, 1188–1193.

(12) McIntosh, J. A., Donia, M. S., Nair, S. K., and Schmidt, E. W. (2011) Enzymatic basis of ribosomal peptide prenylation in cyanobacteria. *J. Am. Chem. Soc.* 133, 13698–13705.

(13) Lee, J., Hao, Y., Blair, P. M., Melby, J. O., Agarwal, V., Burkhardt, B. J., Nair, S. K., and Mitchell, D. A. (2013) Structural and functional insight into an unexpectedly selective N-methyltransferase involved in plantazolicin biosynthesis. *Proc. Natl. Acad. Sci. U.S.A.* 110, 12954–12959.

(14) McIntosh, J. A., Donia, M. S., and Schmidt, E. W. (2009) Ribosomal peptide natural products: Bridging the ribosomal and nonribosomal worlds. *Nat. Prod. Rep.* 26, 537–559.

(15) Milne, J. C., Roy, R. S., Eliot, A. C., Kelleher, N. L., Wokhlu, A., Nickels, B., and Walsh, C. T. (1999) Cofactor requirements and reconstitution of microcin B17 synthetase: A multienzyme complex that catalyzes the formation of oxazoles and thiazoles in the antibiotic microcin B17. *Biochemistry* 38, 4768–4781.

(16) Dunbar, K. L., and Mitchell, D. A. (2013) Insights into the mechanism of peptide cyclodehydrations achieved through the chemoenzymatic generation of amide derivatives. *J. Am. Chem. Soc.* 135, 8692–8701.

(17) Melby, J. O., Dunbar, K. L., Trinh, N. Q., and Mitchell, D. A. (2012) Selectivity, directionality, and promiscuity in peptide processing from a *Bacillus* sp. Al Hakam cyclodehydratase. *J. Am. Chem. Soc.* 134, 5309–5316.

(18) McIntosh, J. A., Donia, M. S., and Schmidt, E. W. (2010) Insights into heterocyclization from two highly similar enzymes. *J. Am. Chem. Soc.* 132, 4089–4091.

(19) Schmidt, E. W., Nelson, J. T., Rasko, D. A., Sudek, S., Eisen, J. A., Haygood, M. G., and Ravel, J. (2005) Patellamide A and C biosynthesis by a microcin-like pathway in *Prochloron didemni*, the cyanobacterial symbiont of *Lissoclinum patella*. *Proc. Natl. Acad. Sci. U.S.A.* 102, 7315–7320.

(20) Kelleher, N. L., Hendrickson, C. L., and Walsh, C. T. (1999) Posttranslational heterocyclization of cysteine and serine residues in the antibiotic microcin B17: Distributivity and directionality. *Biochemistry* 38, 15623–15630.

(21) Donia, M. S., Ravel, J., and Schmidt, E. W. (2008) A global assembly line for cyanobactins. *Nat. Chem. Biol.* 4, 341–343.

(22) Crone, W. J. K., Leeper, F. J., and Truman, A. W. (2012) Identification and characterisation of the gene cluster for the anti-MRSA antibiotic bottromycin: Expanding the biosynthetic diversity of ribosomal peptides. *Chem. Sci.* 3, 3516–3521.

(23) Gomez-Escribano, J. P., Song, L. J., Bibb, M. J., and Challis, G. L. (2012) Posttranslational beta-methylation and macrolactamidation in the biosynthesis of the bottromycin complex of ribosomal peptide antibiotics. *Chem. Sci.* 3, 3522–3525.

(24) Hou, Y., Tianero, M. D., Kwan, J. C., Wyche, T. P., Michel, C. R., Ellis, G. A., Vazquez-Rivera, E., Braun, D. R., Rose, W. E., Schmidt, E. W., and Bugni, T. S. (2012) Structure and biosynthesis of the antibiotic bottromycin D. *Org. Lett.* 14, 5050–5053.

(25) Huo, L., Rachid, S., Stadler, M., Wenzel, S. C., and Muller, R. (2012) Synthetic biotechnology to study and engineer ribosomal bottromycin biosynthesis. *Chem. Biol.* 19, 1278–1287.

(26) Sonnhammer, E. L., Eddy, S. R., and Durbin, R. (1997) Pfam: a comprehensive database of protein domain families based on seed alignments. *Proteins: Struct., Funct., Bioinf.* 28, 405–420.

(27) Finking, R., and Marahiel, M. A. (2004) Biosynthesis of nonribosomal peptides. *Annu. Rev. Microbiol.* 58, 453–488.

(28) Agarwal, V., Pierce, E., McIntosh, J., Schmidt, E. W., and Nair, S. K. (2012) Structures of cyanobactin maturation enzymes define a family of transamidating proteases. *Chem. Biol.* 19, 1411–1422.

(29) Koehnke, J., Bent, A., Houssen, W. E., Zollman, D., Morawitz, F., Shirran, S., Vendome, J., Nneoyiege, A. F., Trembleau, L., Botting, C. H., Smith, M. C., Jaspars, M., and Naismith, J. H. (2012) The

mechanism of patellamide macrocyclization revealed by the characterization of the PatG macrocyclase domain. *Nat. Struct. Mol. Biol.* 19, 767–772.

(30) Massey, V. (1991) A simple method for the determination of redox potentials. In *Flavins and Flavoproteins* (Curti, B., Ronchi, S., and Zanetti, G., Eds.) pp 59–66, Walter de Gruyter, New York.

(31) Martin, R. B., Lowey, S., Elson, E. L., and Edsall, J. T. (1959) Hydrolysis of 2-methyl-delta-2-thiazoline and its formation from N-acetyl-beta-mercaptoethylamine. Observations on an N-S acyl shift. *J. Am. Chem. Soc.* 81, 5089–5095.

(32) Martin, R. B., and Parcell, A. (1961) Hydrolysis of 2-methyl-delta-oxazoline. An intramolecular O-N-acetyl transfer reaction. *J. Am. Chem. Soc.* 83, 4835–4838.

(33) Lee, M. V., Ihnken, L. A., You, Y. O., McClerren, A. L., van der Donk, W. A., and Kelleher, N. L. (2009) Distributive and directional behavior of lantibiotic synthetases revealed by high-resolution tandem mass spectrometry. *J. Am. Chem. Soc.* 131, 12258–12264.

(34) Gonzalez, D. J., Lee, S. W., Hensler, M. E., Markley, A. L., Dahesh, S., Mitchell, D. A., Bandeira, N., Nizet, V., Dixon, J. E., and Dorrestein, P. C. (2010) Clostridiolysin S, a post-translationally modified biotoxin from *Clostridium botulinum*. *J. Biol. Chem.* 285, 28220–28228.

(35) Petushkov, V. N., Gibson, B. G., and Lee, J. (1995) Properties of recombinant fluorescent proteins from *Photobacterium leiognathi* and their interaction with luciferase intermediates. *Biochemistry* 34, 3300–3309.

(36) Visser, A. J., and Lee, J. (1982) Association between lumazine protein and bacterial luciferase: Direct demonstration from the decay of the lumazine emission anisotropy. *Biochemistry* 21, 2218–2226.

(37) Deane, C. D., Melby, J. O., Molohon, K. J., Susarrey, A. R., and Mitchell, D. A. (2013) Engineering unnatural variants of plantazolicin through codon reprogramming. *ACS Chem. Biol.* 8, 1998–2008.

(38) Mitchell, D. A., Lee, S. W., Pence, M. A., Markley, A. L., Limm, J. D., Nizet, V., and Dixon, J. E. (2009) Structural and functional dissection of the heterocyclic peptide cytotoxin streptolysin S. *J. Biol. Chem.* 284, 13004–13012.

(39) Eicher, T., Hauptmann, S., and Speicher, A. (2003) *The Chemistry of Heterocycles: Structure, Reactions, Syntheses, and Applications*, 2nd ed., p 149, Wiley-VCH, Weinheim, Germany.